







# Chapter 1

## Heavy Neutral Leptons

Neutrino oscillation is the key evidence suggesting that neutrinos have mass, a phenomenon that cannot currently be explained by the Standard Model (SM). This motivates an additional right-handed neutrino state that allows for the construction of the Dirac and/or Majorana mass term of neutrinos. If the new state is very heavy, it can potentially provide a new mass generation mechanism to explain the lightness of neutrinos. The heaviness of this new state compared to neutrinos gains it the name *Heavy Neutral Lepton* (HNL). HNLs are proposed to interact with SM gauge bosons, allowing them to be produced and decay via SM gauge interactions. This leads to the focus of this work on the search for HNLs in the mass range of the order  $\mathcal{O}(100)$  MeV that are produced from the Booster Neutrino Beam and then decay into SM observables inside the Short-Baseline Near Detector at Fermilab.

The first chapter here provides an overview on the theory of HNLs and a summary of search results for their existence. In Section 1.1, the motivation of HNLs as a minimal extension to the SM is presented. Section 1.2 provides the explanation for the production mechanism of HNLs from meson decays. Following this, Section 1.3 covers the details of HNL decays into SM observables. Section 1.4 then summarises the existing upper limits on the mixing and mass phase space of HNLs through two different experimental methods: peak searches and decay searches. Finally, Sec. 1.5 provides some brief concluding remarks.

## 1.1 Motivation of Heavy Neutral Leptons

The phenomenon of three-flavour neutrino oscillation is well-established. Active neutrinos are produced and detected as their flavour states  $\nu_\mu$ ,  $\nu_e$  and  $\nu_\tau$  and the neutrino oscillation describes the neutrino flavour states changing from one flavour to another as the neutrinos propagate some distances. Neutrino oscillation directly implies the existence of non-zero mass for at least two out of the three neutrino states. Whilst the Standard Model (SM) of particle physics has proved extremely successful, unfortunately, it currently provides no mechanism for the mass generation of neutrinos. The absence of a right-handed chiral partner to the left-handed chiral neutrino means that no Dirac mass term can be built via the Yukawa coupling of the Higgs to the opposite chirality fields.

This motivates the introduction of a right-handed neutrino such that the neutrino mass can be constructed using the same recipe as all other SM particles. The Dirac mass term in the neutrino Lagrangian after spontaneous symmetry breaking is as follows [1]

$$\mathcal{L}_D = -m_D(\bar{\nu}_L \nu_R + \bar{\nu}_R \nu_L) \quad (1.1)$$

where  $m_D = Yv/\sqrt{2}$  is the Dirac mass,  $Y$  is the Yukawa coupling,  $v$  is the Higgs vacuum expectation value, and the subscript  $R$  and  $L$  denotes the right and left chiral state of the  $\nu$  neutrino and  $\bar{\nu}$  anti-neutrino field. While the Dirac mass term requires the existence of both left and right-handed chiral states, the Majorana mass term was proposed by Ettore Majorana in 1937 requiring only one chiral state [2]. Under the condition that a particle is its own antiparticle, the charge conjugation operator  $C$  can be applied to  $\nu_R$  such that  $\nu_R^C = C\bar{\nu}_R^T$ , where the resulting  $\nu_R^C$  has the correct properties to be used in place of  $\nu_L$  in Eq. 1.1 [3]. The construction of the Majorana state violates the charge conservation and is forbidden for any other SM particles except for neutrinos due to their neutral charges. In this case, the Majorana mass term in the neutrino Lagrangian is as follows [3]

$$\mathcal{L}_M = -\frac{1}{2}M(\bar{\nu}_R^C \nu_R + \bar{\nu}_R \nu_R^C) \quad (1.2)$$

where  $M$  is the Majorana mass. The factor of a half is introduced to account for double counting since the term  $\bar{\nu}_R^C$  and  $\nu_R^C$  are not independent.

A right-handed neutral state provides a hypothetical neutrino mass mechanism not only via the Dirac or the Majorana mass term but also via combining both mass terms. A

## 1.1 Motivation of Heavy Neutral Leptons

---

generalised Lagrangian in this case is as follows [1]

$$\mathcal{L}_{DM} = -\frac{1}{2}[m_D \bar{\nu}_L \nu_R + m_D \bar{\nu}_R^C \nu_L^C + M \bar{\nu}_R^C \nu_R] + h.c. \quad (1.3)$$

The Lagrangian presented here allows for the seesaw mechanism to construct the physical masses of active neutrinos assuming the Majorana mass term is much larger than the Dirac mass term,  $M \gg m_D$  [1, 4]. Under the assumption of only two neutrino states for simplicity, the seesaw mechanism would give the mass of a left-handed neutrino state  $m_\nu \approx \frac{m_D^2}{M}$  and a right-handed neutrino state  $m_N \approx M$ , such that the heaviness of  $m_N$  suppresses the physical mass of the left-handed neutrino  $m_\nu$ . Thus, a right-handed heavy neutrino state is a very attractive addition to the SM as an answer to the neutrino mass mechanism, explaining the extreme lightness of active neutrinos.

The neutral nature of right-handed neutrinos requires all SM charges to be zero implying that they do not interact directly via the strong, electromagnetic, or weak forces. These weaker-than-weak right-handed particles are often referred to as *sterile neutrinos*. The only direct coupling to the new sterile state is the neutrino-Higgs interaction. This leads to mixing-mediated interactions with SM gauge bosons, allowing them to be produced and decay via SM gauge interactions with a rate suppressed by the mixing [5]. The mass range of sterile neutrinos can span over many orders of magnitudes, and the number of flavour or mass states is unconstrained.

In the mass range of the order  $\mathcal{O}(1)$  eV, they are known as *light* sterile neutrinos and are proposed to participate in *oscillation* with active neutrinos. Over a short baseline distance, the addition of a single light sterile neutrino to neutrino *oscillation* might enhance or reduce the number of observed neutrino interactions for a given channel. Particularly, this model can explain the outstanding anomaly observed by the LSND and MiniBooNE experiments, where an excess of  $\nu_e$  and  $\bar{\nu}_e$  interactions was measured at low energy [6–8].

In the mass range  $> \mathcal{O}(10)$  eV, sterile neutrinos are now considered *heavy* since their masses are significantly more massive compared to active neutrinos. This gains them the name *Heavy Neutral Leptons* (HNLs). HNLs do not participate in *oscillation* with active neutrinos due to coherence loss [5]. As a consequence of being heavier than active neutrinos, the wave packet of HNLs moves much slower compared to that of active neutrinos and immediately undergoes propagation decoherence. Instead, HNLs are proposed to travel over some *distances* before decaying into SM observables.

Different theoretical models of HNLs have been developed, and a comprehensive review can be found in Ref. [8]. In the search for HNLs presented here, the existence of HNLs

will be explored in a minimal way by assuming an addition of a single HNL to the SM. From a generic phenomenological approach, an HNL can be added to the SM by extending the Pontecorvo-Maki-Nakagawa-Sakata (PMNS) matrix. The PMNS matrix, describing the mixing of the SM neutrino flavour eigenstate  $\nu_\alpha$  ( $\alpha = e, \mu, \tau$ ), and the mass eigenstate  $\nu_i$  ( $i = 1, 2, 3$ ), is as follows

$$U_{PMNS} = \begin{pmatrix} U_{e1} & U_{e2} & U_{e3} \\ U_{\mu1} & U_{\mu2} & U_{\mu3} \\ U_{\tau1} & U_{\tau2} & U_{\tau3} \end{pmatrix} \quad (1.4)$$

The flavour eigenstate  $\nu_\alpha$  **undergoes weak interaction**, whilst the mass eigenstate  $\nu_i$  describes the neutrino propagation in space and time. For the addition of a single right-handed neutrino with mass  $m_N$ , the PMNS matrix can be extended to describe the mass mixing between SM neutrinos and the new flavour eigenstate  $N$  as follows

$$U_{PMNS}^{Extended} = \begin{pmatrix} U_{e1} & U_{e2} & U_{e3} & U_{e4} \\ U_{\mu1} & U_{\mu2} & U_{\mu3} & U_{\mu4} \\ U_{\tau1} & U_{\tau2} & U_{\tau3} & U_{\tau4} \\ U_{N1} & U_{N2} & U_{N3} & U_{N4} \end{pmatrix} \quad (1.5)$$

where the index 4 is reserved **as** the new mass eigenstate. Then, the flavour eigenstate  $\nu_\alpha$  of SM neutrinos can be written as the linear combination of the mass eigenstate  $\nu_i$  and the HNL flavour eigenstate  $N$  as follows

$$\nu_\alpha = \sum_i U_{\alpha i} \nu_i + U_{\alpha 4} N \quad (1.6)$$

where the mixing  $U_{\alpha i}$  ( $\alpha = e, \mu, \tau$  and  $i = 1, 2, 3$ ) are elements of the SM PMNS matrix, and the mixing  $U_{\alpha 4}$  are the extension. For simplicity, this work only considers an HNL coupling to only one flavour at a time, such that at most one of the three mixing  $U_{e4}$ ,  $U_{\mu4}$  and  $U_{\tau4}$  is non-zero.

## 1.2 Production of Heavy Neutral Leptons

In any SM neutrino production processes, HNLs can be produced in place of neutrinos with a rate suppressed by the mixing  $|U_{\alpha 4}|^2$ , if kinematically allowed. Fig. 1.1a illustrates the two-body decay of a charged kaon  $K^+$  producing a muon neutrino  $\nu_\mu$  and Fig. 1.1b illustrates the substitution of the  $\nu_\mu$  with an HNL  $N$  having  $L = +1$  mediated by the mixing  $|U_{\alpha 4}|^2$ . This implies that HNLs can be probed from the Booster Neutrino Beam (BNB), which

## 1.2 Production of Heavy Neutral Leptons

is an **abundance** source of mesons and will be further detailed in Sec. 3.3. Since the BNB is primarily made up of positively charged mesons, the following section will focus on the parent meson  $K^+$  and  $\pi^+$ .

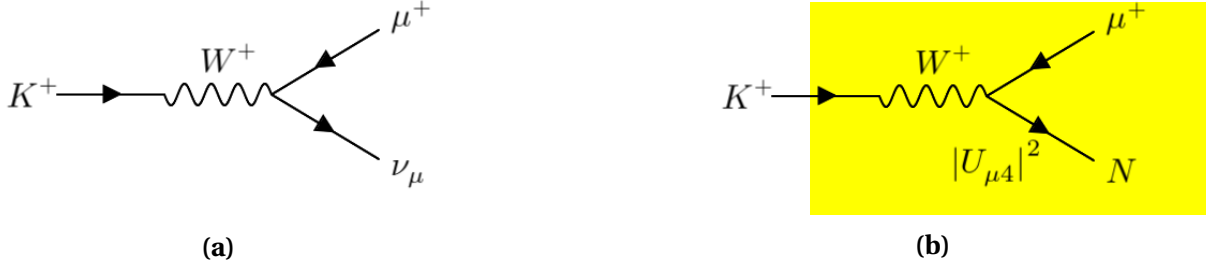


**Fig. 1.1** Feynman diagrams of (a)  $K^+ \rightarrow \mu^+ \nu_\mu$  and (b)  $K^+ \rightarrow \mu^+ N$ .

In general, the branching ratio  $Br(m^+ \rightarrow l_\alpha^+ N)$  of a two-body decay of a charged meson  $m^+$  into a lepton  $l_\alpha^+$  ( $\alpha = e, \mu, \tau$ ) and an HNL  $N$  can be expressed in terms of the analogous branching ratio into an SM neutrino as follows [9]

$$Br(m^+ \rightarrow l_\alpha^+ N) = Br(m^+ \rightarrow l_\alpha^+ \nu_\alpha) \left( \frac{|U_{\alpha 4}|^2}{1 - |U_{\alpha 4}|^2} \right) \rho_N \left( \frac{m_{l_\alpha}^2}{m_{m^+}^2}, \frac{m_N^2}{m_{m^+}^2} \right) \quad (1.7)$$

where  $Br(m^+ \rightarrow l_\alpha^+ \nu_\alpha)$  is the branching ratio of the charged lepton  $m^+$  decaying into a lepton  $l_\alpha^+$  and an SM neutrino  $\nu_\alpha$ ,  $m_{m^+}$  is the mass of the charged meson,  $m_{l_\alpha}$  is the mass of the daughter lepton and  $m_N$  is the mass of the daughter HNL. The kinematic factor  $\rho_N$  accounts for the available phase space of the daughter HNL in the decay and has the complete expansion as follows [9]

$$\rho_N(x, y) = \frac{(x + y - (x - y)^2) \sqrt{1 + x^2 + y^2 - 2(x + y + xy)}}{x(1 - x)^2} \quad (1.8)$$

where  $x = m_{l_\alpha}^2 / m_{m^+}^2$  and  $y = m_N^2 / m_{m^+}^2$ .

Fig. 1.2 depicts the kinematic factor  $\rho_N$  of the HNL production compared to the analogous SM neutrino production as a function of the HNL mass. Four HNL production channels that are probable at the BNB are shown: (1)  $K^+ \rightarrow N e^+$  in the dashed red line, (2)  $K^+ \rightarrow N \mu^+$  in the solid pink line, (3)  $\pi^+ \rightarrow N e^+$  in the dashed dark blue line and (4)  $\pi^+ \rightarrow N \mu^+$  in the solid light blue line. Production channels associated with the  $\tau$ -flavour mixing are not shown since they are kinematically forbidden **at the BNB**. The kinematic factor for each illustrated channel is constrained by the available mass after the two-body decay of the parent meson. The upper limit of the HNL mass is therefore  $m_N = m_{m^+} - m_{l_\alpha}$  ( $\alpha = e, \mu$ ), as shown by the

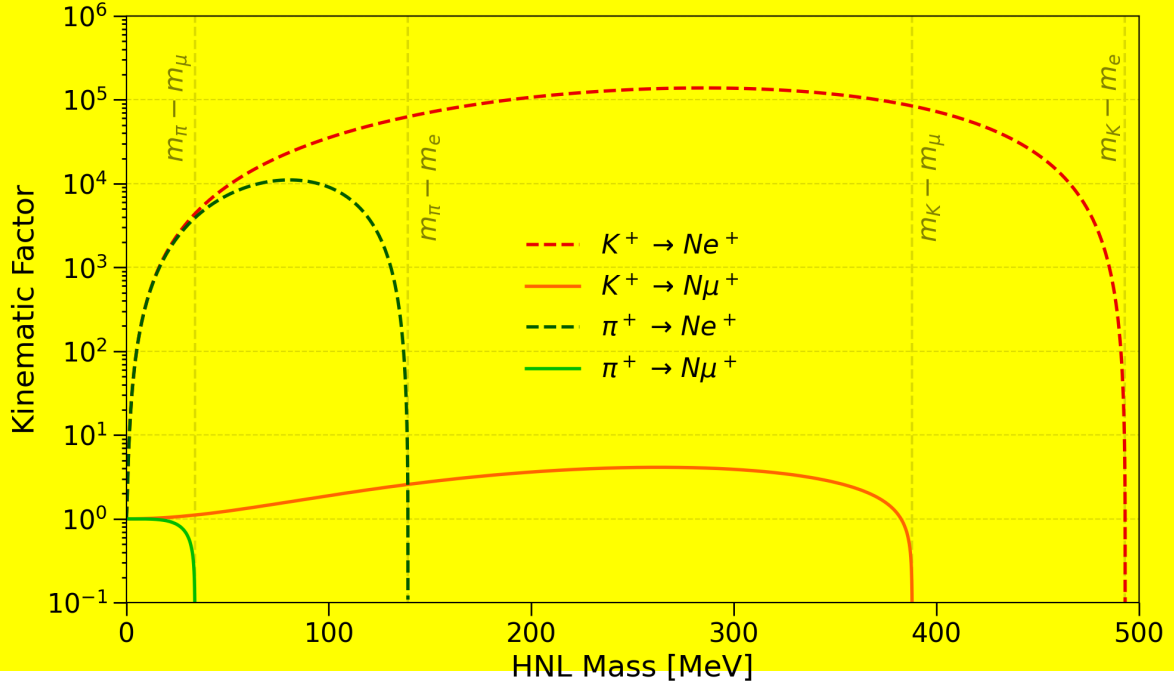


**Fig. 1.2** Plot showing the kinematic factor of the HNL production from meson decays as compared to the analogous SM neutrino production.

vertical grey lines. Here it can be seen that the HNL production from  $\pi^+$  decays limits the HNL mass to  $< 140$  MeV while the HNL production from  $K^+$  decays allows for the HNL mass up to 495 MeV. Thus, the search for HNLs presented here focuses on the HNL production channel from  $K^+$  to probe mass as high as 495 MeV.

Furthermore, the magnitude of the kinematic factor of the HNL production shown in Fig. 1.2 is larger than 1 as compared to the analogous SM production. This is because of the helicity suppression observed in mesons decaying into an SM neutrino having an opposite effect for mesons decaying into an HNL [9]. Instead, it is helicity *enhancement* due to HNLs being massive. For the HNL production channel *interested in this work*, a significant enhancement is evident for the production rate of  $K^+ \rightarrow e^+ N$  being increased by a factor of  $10^5$ . On the other hand, the kinematic factor of  $K^+ \rightarrow \mu^+ N$  unfortunately only peaks at 4, implying a negligible enhancement in the production rate.



### 1.3 Decay Channels of Heavy Neutral Leptons

For HNLs to be detected, they are hypothesised to be able to decay into SM observables [9]. The proposed lifetime of HNLs should be sufficient so that an HNL produced from the BNB **must** survive long enough to reach the detector and then decay in flight. At the mass range  $< 495$  MeV, the kinematically-allowed decay channels of an HNL are **as follows** [5]

$$\begin{aligned} N \rightarrow e^- \pi^+, \quad N \rightarrow \mu^- \pi^+, \quad N \rightarrow \nu \pi^0, \quad N \rightarrow \nu \gamma, \\ N \rightarrow \nu e^- e^+, \quad N \rightarrow \nu \mu^- \mu^+, \quad N \rightarrow \nu \mu^- e^+, \quad N \rightarrow \nu \nu \nu. \end{aligned} \quad (1.9)$$

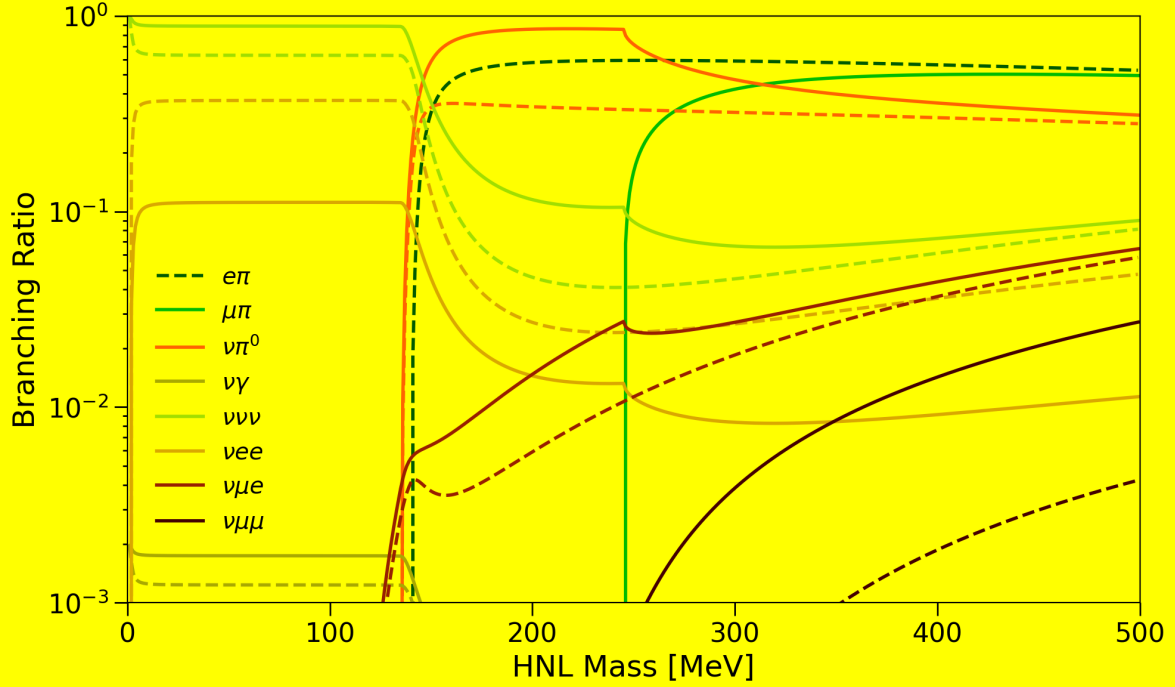
These decay channels **here** conserve the lepton number under the assumption that HNLs are Dirac particles with  $L = +1$ . If HNLs are Majorana particles, such that the lepton number conservation is violated, then the charge conjugates for these decays that would be forbidden in the Dirac case are **now** allowed.

Fig. 1.3 depicts **branching ratios** of decay channels shown in Eq. 1.9, as a function of the HNL mass. Solid lines are branching ratios via the  $\mu$ -flavour mixing ( $[U_{e4} : U_{\mu 4} : U_{\tau 4}] = [0 : 1 : 0]$ ) and dashed lines are branching ratios via the  $e$ -flavour mixing ( $[U_{e4} : U_{\mu 4} : U_{\tau 4}] = [1 : 0 : 0]$ ). The branching ratios were plotted referencing decay widths from Ref. [5, 10, 11]. Decay widths of HNLs have been derived independently across various literature sources and an overview of **discrepancies** is summarised in Ref. [11]. The sources used here have been found to be in good agreement with each other.

For  $m_N < 135$  MeV, the dominant branching ratio occurs in the channel  $N \rightarrow \nu \nu \nu$  as shown by the light green lines. However, this channel is almost unobservable since the detection of SM neutrinos relies on the already-small cross section of neutrino scattering with the detector material. The other two channels in this mass range are  $N \rightarrow \nu e^- e^+$  and  $N \rightarrow \nu \gamma$ , as shown by the light pink and grey lines. The channel  $N \rightarrow \nu \gamma$  is highly suppressed compared to the channel  $N \rightarrow \nu e^- e^+$ , and thus, the final state **of  $e^- e^+$**  pair provides the best sensitivity within this mass range.

**For  $m_N > 135$  MeV, an HNL has sufficient mass** to decay into either a neutral pion ( $m_{\pi^0} = 135$  MeV) or a charged pion ( $m_{\pi^\pm} = 140$  MeV). For the  $e$ -flavour mixing, the channel  $N \rightarrow e^- \pi^+$  dominates over the channel  $N \rightarrow \nu \pi^0$  across the mass range from 135 to 495 MeV, as shown by the dashed dark blue and dashed pink line respectively. In the case of the  $\mu$ -flavour mixing, the leading channel within the mass range of  $135 < m_N < 245$  MeV is  $N \rightarrow \nu \pi^0$  as shown by the solid pink line. Beyond  $m_N > 245$  MeV, equivalent to the mass of a muon and a charged pion, the dominant decay channel begins to shift to the

channel  $N \rightarrow \mu^- \pi^+$  as shown by the solid blue line. Finally, both channels  $N \rightarrow \nu \mu^- e^+$  and  $N \rightarrow \nu \mu^- \mu^+$  are not competitive compared to any other channels at the same mass value.



**Fig. 1.3** Plot showing the branching ratio of probable decay channels of an HNL produced from the BNB.

Based on the assessment above it was decided in this work to focus on searching for HNLs through the decay channel  $N \rightarrow \nu \pi^0$ , which will be covered in Chapter 8 and 9. This is the leading channel of the  $\mu$ -flavour mixing within the mass range of  $135 < m_N < 245$  MeV. Sensitivity in the same mass range of the  $e$ -flavour mixing has been extensively explored by many experiments as summarised by Ref. [8]. The decay width for the  $N \rightarrow \nu \pi^0$  channel as taken from Ref. [11] is as follows

$$\Gamma(N \rightarrow \nu \pi^0) = \frac{G_F^2 m_N^3}{32\pi} f_\pi^2 |U_{\mu 4}|^2 \left( 1 - \left( \frac{m_{\pi^0}}{m_N} \right)^2 \right)^2 \quad (1.10)$$

where  $G_F$  is the Fermi constant,  $f_\pi$  is the pion decay constant and  $m_{\pi^0}$  is the mass of a neutral pion. It is noted that the equivalent equations from Ref. [5, 10] contain an additional factor of 2 in the denominator. Eq. 1.10 was chosen from Ref. [11] since the source is more recently dated.

Fig. 1.4a shows the diagram of the HNL decaying into the final state  $\nu \pi^0$ . The SM neutrino is expected to leave no detectable signatures due to their very small scattering

### 1.3 Decay Channels of Heavy Neutral Leptons

**cross sections.** Meanwhile, the neutral pion is a particle made up of the superposition of the quark pair  $u\bar{u}$  and  $d\bar{d}$ . The annihilation **of quark and antiquark** makes it a very short-lived particle with a mean lifetime of  $8.52 \pm 0.18 \times 10^{-17}$  s [12]. The neutral pion **decay** has been measured to decay into two photons  $98.823 \pm 0.034\%$  of the time. Fig. 1.4b shows the Feynman diagram for **the described** decay. The photon pair results in a clear signature inside a Liquid Argon Time Projection Chamber (LArTPC): two electromagnetic showers without any associated hadronic activities at the decay vertex. This signal topology will face very challenging background separation from some SM neutrino channels also containing a  $\pi^0$  in the final state. As described in more detail in Chapter 8, differences in the final state kinematics from the HNL signal to the SM neutrino background enable an effective separation.

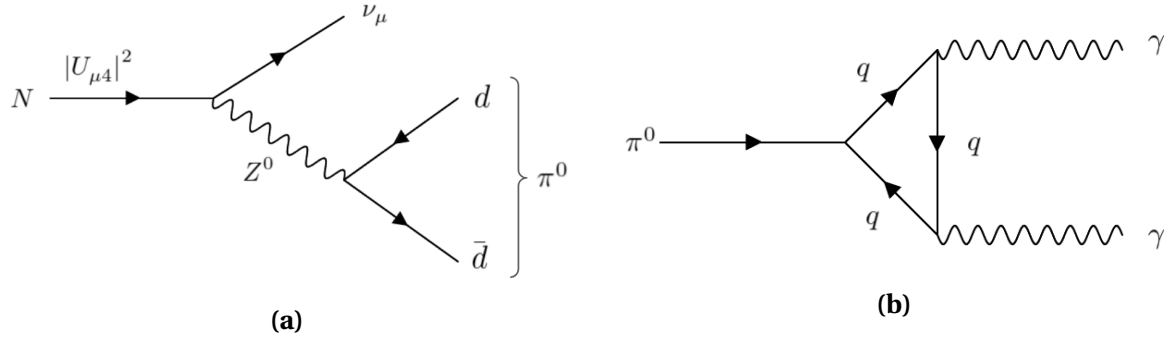


**Fig. 1.4** Feynman diagrams of (a)  $N \rightarrow \nu\pi^0$  and (b)  $\pi^0 \rightarrow \gamma\gamma$ .

As previously discussed in Sec. 1.2, HNLs can be either Dirac or Majorana particles in nature. The difference between Dirac and Majoranan HNLs is not only the lepton number conservation but also the polarisation of the decay products. For the neutral current final state  $\nu\pi^0$ , Majoranan HNLs decay isotropically, whereas in the case of Dirac HNLs, the angular distribution of the daughter particles is no longer isotropic. The helicity of the daughter neutrino determines the direction of the daughter neutral pion **and the** angular distributions of the two charge conjugate final states,  $\nu\pi^0$  and  $\bar{\nu}\pi^0$ , add up to an isotropic distribution [13]. As the neutrino is undetectable, the observed angular distribution of the neutral pion is expected to be insufficient to determine the Dirac or Majorana nature of HNLs. For simplicity in this search for HNLs via the channel  $\nu\pi^0$ , it is therefore assumed that HNLs are Majorana particles.

## 1.4 Previous Experimental Searches For Heavy Neutral Leptons

Searches for HNLs have been conducted by various experiments over the decades across a wide range of mass. Oscillation experiments and precise  $\beta$  decay experiments have probed HNLs in the mass range between eV and keV, neutrino beam dump experiments have targeted the MeV-scale HNLs and collider experiments have primarily explored HNLs with masses in the GeV-scale and above. To date, no evidence of HNL existence has been found, and thus, experiments have set upper limits on the mixing  $|U_{\alpha 4}|^2$  ( $\alpha = e, \mu, \tau$ ). Commonly, the contour on the experiment sensitivity is expressed in terms of the mixing  $|U_{\alpha 4}|^2$  as a function of the HNL mass.

Here, current experimental limits on HNLs around  $\mathcal{O}(100 \text{ MeV})$  are presented, focusing specifically on the mass range of  $0 < m_N < 265 \text{ MeV}$ , which is relevant to the final states  $\nu\pi^0$ . In this mass range, two key experimental methods are used, so-called peak searches and decay searches. Peak searches probe only the production rate of HNLs, whereas decay searches probe both production and decay rates. Fig. 1.5 summarises the presented upper limits at 90% confidence level (C.L.) from both experimental methods, with details on individual limit to be discussed in Sec. 1.4.1 and 1.4.2.

### 1.4.1 Peak Searches

Peak search experiments measure the energy spectrum resulting from the decay of meson decay that would produce an HNL. Typically, the two-body leptonic decay of a meson is modelled as  $m \rightarrow l + \text{Missing}$ , where  $m$  is the parent meson, a pion or a kaon, and  $l$  is the daughter particle, a pion or a lepton [14]. The *missing* decay products are attributed to either HNLs or SM neutrinos. HNLs are expected to exit the detector before decaying, whereas SM neutrinos escape the detector before interacting, serving as the primary background for this search. Since the momenta of  $m$  and  $l$  are precisely measured, the missing invariant mass can therefore be derived as  $m_{\text{miss}}^2 = (P_m - P_l)^2$ , where  $P_m$  and  $P_l$  are the 4-momenta of the parent and daughter particle. Given the near-zero mass of SM neutrinos, the mass of the daughter HNL can be treated as  $m_N = m_{\text{miss}}$ . Consequently, an excess over the background at  $m_{\text{miss}}$  potentially indicates the existence of HNLs.

To infer the upper limits on the mixing parameter, the flavour  $\alpha$  ( $\alpha = \mu, e$ ) of the daughter lepton determines the flavour of the mixing  $|U_{\alpha 4}|^2$ , and the amplitude of the decay spectrum at  $m_{\text{miss}}$  determines the upper limit. Limits placed by the peak searches are insensitive to

## 1.4 Previous Experimental Searches For Heavy Neutral Leptons

the Dirac or Majorana nature of HNLs as **it** does not impact the kinematics of the meson decay. For the mixing  $|U_{\mu 4}|^2$ , the most competitive limits have been established by the following experiments on the pion and kaon decay spectrum, and are plotted in Fig. 1.5 as dashed lines.

### Pion Decay Spectrum Peak Searches

- **SIN** (Swiss Institute for Nuclear Research) performed a **peak search using stopped** positive pions decay via the channel  $\pi^+ \rightarrow \mu^+ + \text{Missing}$ , with a scintillator in 1981 and a germanium detector in 1987. The pion enabled **probing HNLs** within the low mass range of  $\mathcal{O}(10 \text{ MeV})$ . Upper limits of  $|U_{\mu 4}|^2$  were placed in the mass range 1–20 MeV at  $10^{-4}$  [15–17].
- The **PIENU** collaboration at **TRIUMF** also searched for HNLs using **stopped** pions. The most recent result in 2019 set the most stringent limits on  $|U_{\mu 4}|^2$  at  $10^{-5}$  in the mass range of 15–34 MeV, extending beyond the result reported by SIN [18].

### Kaon Decay Spectrum Peak Searches

- The **KEK** collaboration conducted an experiment known as E89, which aimed to search for HNLs using the **muon range spectrum** resulting from **stopped** kaon decays during 1981–1982. Following this, experiment E104 in 1983 was carried out with an improved momentum resolution and background suppression. The kaons were produced using a 0.5 GeV proton beam, and  $3 \times 10^6$  muons from kaon decays were analysed using a magnetic spectrograph. The E89 experiment result set limits on  $|U_{\mu 4}|^2$  between  $10^{-4}$ – $10^{-6}$  within the mass range of 70–300 MeV. Additionally, the combined results from the E89 and E104 experiments extended the sensitivity towards the lower mass range between 45–300 MeV, although these findings were unpublished at the time of writing and therefore plotted as the dotted line in Fig. 1.5 [19–21].
- The **E949** collaboration at Brookhaven National Laboratory performed a kaon decay experiment using 21.5 GeV protons in 2002. The analysis on the decays of  $2 \times 10^{21}$  **stopped** kaons set **limits on  $|U_{\mu 4}|^2$  at  $10^{-7}$ – $10^{-9}$**  within the mass range of 175–300 MeV [22].
- The **NA62** collaboration, a kaon decay experiment at the CERN super proton synchrotron, analysed  $10^8$  stopped kaons from 400 GeV protons extracted from the synchrotron. The first results from a data set in 2015 set upper limits on  $|U_{\mu 4}|^2$  at

$10^{-7}$ – $10^{-6}$  for the HNL mass between 250–373 MeV. Updated results using a larger dataset collected in 2016–2018 significantly improved the limits by an order of magnitude to  $10^{-8}$ – $10^{-7}$ , and extended the mass range to 200–384 MeV [23, 24].

### 1.4.2 Decay Searches

Decay searches look for decay products from HNLs. HNLs are hypothesised to be produced outside of the detector and then decay in flight into SM observables inside the detector. Different combinations of HNL production and decay channels yield different observed event rates of the decay products. The flavour of the HNL production and decay channel both determine the flavour of the mixing  $|U_{\alpha 4}|^2$  and the observed event rate determines the upper limit on the mixing.

Historically, decay searches have been performed in beam-dump experiments, which were designed explicitly to suppress SM background thereby enabling the search for rare decay processes. Recently, modern neutrino oscillation experiments have emerged as competitive beam-dump experiments alongside their neutrino physics programme. This is due to the resolution enhancement in their detection technologies that enable excellent SM background rejection, of which the **Short-Baseline Near Detector** is a prime example to be further detailed in this work. For the mixing  $|U_{\mu 4}|^2$  within the mass range of 0–265 MeV, the most competitive limits have been set by the following experiments using neutrino beams, and are plotted in Fig. 1.5 as solid lines.

- The CERN **PS191** experiment in 1984 utilised an exposure of 19.2 GeV protons on a beryllium target, generating  $10^{19}$  protons on target (POT). The detector was positioned at 128 m from the target at an off-axis angle of  $2.3^\circ$  to the beam. The detector volume was filled with helium, which was a sparse medium to reduce background rates arising from SM neutrino interactions. The large volume of 216 m<sup>3</sup> provided a high rate of HNL signals. Limits on  $|U_{\mu 4}|^2$  within the mass range of 120–350 MeV were placed at the level of  $10^{-5}$ – $10^{-9}$  [25, 26]. A re-evaluation in 2022 found the limits to be lower than the original published results [27].
- The **NuTeV** collaboration at Fermilab conducted HNL searches in 1996 using a high energy neutrino beam produced by protons accelerated from the Tevatron ring. The dataset comprised an exposure of  $3 \times 10^{18}$  POT with an energy of 800 GeV. HNLs were produced from the  $D$  mesons resulting from proton collisions with the target. This enabled an exploration of the HNL mass up to 2000 MeV, surpassing any other beam-

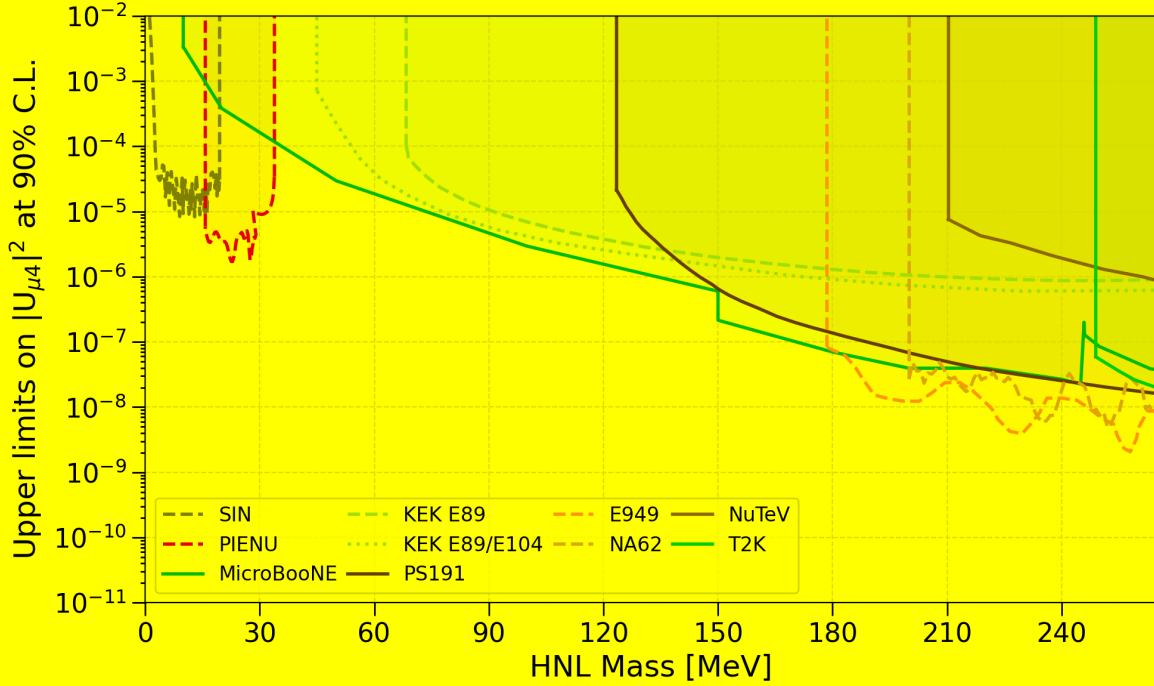


**Fig. 1.5** Plot showing the upper limits on the mixing  $|U_{\mu 4}|^2$  at 90% C.L. for Majoranan HNLs in the mass range of  $0 < m_N < 265$  MeV.

dump experiments described here. The experiment established limits on  $|U_{\mu 4}|^2$  at the level of  $10^{-6}$ – $10^{-7}$  within the mass range of 225–2000 MeV [28].

- The **T2K** collaboration searched for HNLs using their near detector ND280 located off-axis to the beam target at an angle of  $2.04^\circ$ . Only events occurring in the three gaseous TPC volumes were selected to minimise background from SM neutrinos. A kinematic selection was performed on a dataset of  $2 \times 10^{21}$  POT and no signals were observed. The result constrained the mixing  $|U_{\mu 4}|^2$  at the level of  $10^{-8}$ – $10^{-9}$  in the mass range of 250–380 MeV. The limit plotted in Fig. 1.5 is a single-channel limit of  $K^\pm \rightarrow N\mu^\pm$  and  $N \rightarrow \mu^\pm\pi^\pm$ . A more stringent limit on  $|U_{\mu 4}|^2$  was also presented assuming the mixing  $|U_{e 4}|^2$  and  $|U_{\tau 4}|^2$  are non-zero. This allows for a marginalised limit on  $|U_{\mu 4}|^2$  derived from other mixing results, which is not directly comparable here [29].
- The **MicroBooNE** collaboration conducted a series of searches for HNLs using their LArTPC, with the first result in 2020 and subsequent results in 2022 and 2023. The initial analysis was performed using an exposure of  $2 \times 10^{20}$  POT obtained from the on-axis BNB. A special delayed trigger was implemented to identify HNLs arriving at

the detector later than SM neutrinos. Limits on  $|U_{\mu 4}|^2$  were set at  $10^{-7}$  for HNL masses spanning between 260–385 MeV. The latter two searches focused on HNLs arising from **kaons** decays in the NuMI beam absorber, which arrived at the detector at an angle to SM neutrinos from the BNB. The dataset included two runs with an exposure of  $2 \times 10^{20}$  and  $5.01 \times 10^{20}$  POT. The combined results incorporated multiple HNL decay channels, probing a wide mass spectrum between 10–385 MeV. Notably, these recent results set the most stringent limits to date on  $|U_{\mu 4}|^2$  at  $10^{-4}$ – $10^{-7}$  within the mass range of 34–175 MeV, extending the findings from 2019 [30–32].

## 1.5 Concluding Remarks

HNLs are **beyond SM** particles that can provide a natural explanation not just for the mass generation of active neutrinos but also for their extreme lightness. SBND, located only 110 m from the BNB, is capable of detecting HNLs resulting from meson decays in the beam, which then decay in flight inside the detector. Fig. 1.5 provides a summary of existing limits on the mixing  $|U_{\mu 4}|^2$  of HNLs in the mass range of 0–265 MeV, showing that this phase space has been well-explored by various experiments very recently. For SBND to be competitive in this region, a high background rejection rate without comprising signal efficiency must be achieved when performing the kinematic selection. This can be obtained by exploiting **kinematic** observables of HNL decay products for background rejection, including their delay compared to SM neutrinos as well as their boosted kinematics due to HNLs being massive. Toward this goal, novel detection technology and reconstruction techniques of SBND have demonstrated an excellent **resolution in timing, spatial and calorimetry**. The **following Chapter 2 and 3** will provide an overall description of the LArTPC technology, followed by details of the detection technology at SBND.





## References

- [1] M. Thomson, *Modern particle physics* (Cambridge University Press, New York, 2013).
- [2] E. Majorana, “Teoria simmetrica dell’elettrone e del positrone”, [Nuovo Cim. \*\*14\*\*, 171–184 \(1937\)](#).
- [3] C. Giunti et al., *Fundamentals of Neutrino Physics and Astrophysics* (Oxford University Press, Incorporated, 2007).
- [4] S. F. King, “Neutrino mass models”, [Rept. Prog. Phys. \*\*67\*\*, 107–158 \(2004\)](#).
- [5] P. Ballett et al., “MeV-scale sterile neutrino decays at the Fermilab Short-Baseline Neutrino program”, [JHEP \*\*04\*\*, 102 \(2017\)](#).
- [6] A. Aguilar et al. (LSND Collaboration), “Evidence for neutrino oscillations from the observation of  $\bar{\nu}_e$  appearance in a  $\bar{\nu}_\mu$  beam”, [Phys. Rev. D \*\*64\*\*, 112007 \(2001\)](#).
- [7] A. A. Aguilar-Arevalo et al. (MiniBooNE Collaboration), “Significant Excess of Electron-like Events in the MiniBooNE Short-Baseline Neutrino Experiment”, [Phys. Rev. Lett. \*\*121\*\*, 221801 \(2018\)](#).
- [8] M. A. Acero et al., “White Paper on Light Sterile Neutrino Searches and Related Phenomenology”, (2022).
- [9] J. M. Berryman et al., “Searches for Decays of New Particles in the DUNE Multi-Purpose Near Detector”, [JHEP \*\*02\*\*, 174 \(2020\)](#).
- [10] A. Atre et al., “The Search for Heavy Majorana Neutrinos”, [JHEP \*\*05\*\*, 030 \(2009\)](#).
- [11] P. Coloma et al., “GeV-scale neutrinos: interactions with mesons and DUNE sensitivity”, [Eur. Phys. J. C \*\*81\*\*, 78 \(2021\)](#).
- [12] P. A. Zyla et al. (Particle Data Group), “Review of Particle Physics”, [PTEP \*\*2020\*\*, 083C01 \(2020\)](#).
- [13] P. Ballett et al., “Heavy Neutral Leptons from low-scale seesaws at the DUNE Near Detector”, [JHEP \*\*03\*\*, 111 \(2020\)](#).
- [14] O. Goodwin, “Search for Higgs Portal Scalars and Heavy Neutral Leptons Decaying in the MicroBooNE Detector”, PhD thesis (The University of Manchester, 2022).
- [15] R. Abela et al., “Search for an Admixture of Heavy Neutrino in Pion Decay”, [Phys. Lett. B \*\*105\*\*, \[Erratum: Phys.Lett.B 106, 513 \(1981\)\], 263–266 \(1981\)](#).
- [16] R. C. Minehart et al., “Search for Admixtures of Massive Neutrinos in the Decay  $\pi^+ \rightarrow \mu^+ + \bar{\nu}$ ”, [Phys. Rev. Lett. \*\*52\*\*, 804–807 \(1984\)](#).
- [17] M. Daum et al., “Search for admixtures of massive neutrinos in the decay  $\pi^+ \rightarrow \mu^+ + \nu$ ”, [Phys. Rev. D \*\*36\*\*, 2624–2632 \(1987\)](#).

- [18] A. Aguilar-Arevalo et al. (PIENU), “Search for heavy neutrinos in  $\pi \rightarrow \mu \nu$  decay”, [Phys. Lett. B \*\*798\*\*, 134980 \(2019\)](#).
- [19] Y. Asano et al., “Search for a Heavy Neutrino Emitted in  $K^+ \rightarrow \mu^+ \nu$  Neutrino Decay”, [Phys. Lett. B \*\*104\*\*, 84–88 \(1981\)](#).
- [20] R. S. Hayano et al., “Heavy-Neutrino Search Using  $K_{\mu 2}$  Decay”, [Phys. Rev. Lett. \*\*49\*\*, 1305–1309 \(1982\)](#).
- [21] T. Yamazaki et al., “Search for Heavy Neutrinos in Kaon Decay”, in Proc. of the 22nd International Conference on High Energy Physics, Vol. 840719, edited by A. Meyer et al. (1984), p. 262.
- [22] A. V. Artamonov et al. (E949), “Search for heavy neutrinos in  $K^+ \rightarrow \mu^+ \nu_H$  decays”, [Phys. Rev. D \*\*91\*\*, \[Erratum: Phys.Rev.D \*\*91\*\*, 059903 \(2015\)\], 052001 \(2015\)](#).
- [23] E. Cortina Gil et al. (NA62), “Search for heavy neutral lepton production in  $K^+$  decays”, [Phys. Lett. B \*\*778\*\*, 137–145 \(2018\)](#).
- [24] E. Cortina Gil et al. (NA62), “Search for  $K^+$  decays to a muon and invisible particles”, [Phys. Lett. B \*\*816\*\*, 136259 \(2021\)](#).
- [25] G. Bernardi et al., “Search for neutrino decay”, [Physics Letters B \*\*166\*\*, 479–483 \(1986\)](#).
- [26] G. Bernardi et al., “Further limits on heavy neutrino couplings”, [Physics Letters B \*\*203\*\*, 332–334 \(1988\)](#).
- [27] C. A. Argüelles et al., “Heavy neutral leptons below the kaon mass at hodoscopic neutrino detectors”, [Phys. Rev. D \*\*105\*\*, 095006 \(2022\)](#).
- [28] A. Vaitaitis et al. (NuTeV, E815), “Search for neutral heavy leptons in a high-energy neutrino beam”, [Phys. Rev. Lett. \*\*83\*\*, 4943–4946 \(1999\)](#).
- [29] K. Abe et al. (T2K), “Search for heavy neutrinos with the T2K near detector ND280”, [Phys. Rev. D \*\*100\*\*, 052006 \(2019\)](#).
- [30] P. Abratenko et al. (MicroBooNE), “Search for Heavy Neutral Leptons Decaying into Muon-Pion Pairs in the MicroBooNE Detector”, [Phys. Rev. D \*\*101\*\*, 052001 \(2020\)](#).
- [31] P. Abratenko et al. (MicroBooNE), “Search for long-lived heavy neutral leptons and Higgs portal scalars decaying in the MicroBooNE detector”, [Phys. Rev. D \*\*106\*\*, 092006 \(2022\)](#).
- [32] P. Abratenko et al. (MicroBooNE), “Search for heavy neutral leptons in electron-positron and neutral-pion final states with the MicroBooNE detector”, (2023).